Dynamic QTL analysis for developmental behavior of cell wall components and forage digestibility in maize (Zea mays L.)

Kun Li
Institute of Crop Sciences, Chinese Academy of Agricultural Sciences
Xue Yang
Institute of Crop Sciences, Chinese Academy of Agricultural Sciences
Xiaogang Liu
Institute of Crop Sciences, Chinese Academy of Agricultural Sciences
Xiaojiao Hu
Institute of Crop Sciences, Chinese Academy of Agricultural Sciences
Yujin Wu
Institute of Crop Sciences, Chinese Academy of Agricultural Sciences
Qi Wang
Institute of Crop Sciences, Chinese Academy of Agricultural Sciences
Feiqian Ma
Institute of Crop Sciences, Chinese Academy of Agricultural Sciences
Shuqiang Li
Institute of Crop Sciences, Chinese Academy of Agricultural Sciences
Hongwu Wang
Institute of Crop Sciences, Chinese Academy of Agricultural Sciences
Zhifang Liu
Institute of Crop Sciences, Chinese Academy of Agricultural Sciences
Changling Huang (huangchangling@caas.cn)
Institute of Crop Sciences, Chinese Academy of Agricultural Sciences

Research Article

Keywords: Quantitative trait locus, Maize (Zea mays L.), Cell Wall Components, Forage quality

Posted Date: December 17th, 2020

DOI: https://doi.org/10.21203/rs.3.rs-128172/v1

Dynamic QTL analysis for developmental behavior of cell wall components and forage digestibility in maize (*Zea mays* L.)

Kun Li[1, 2, #], Xue Yang[1, 2, #], Xiaogang Liu[1, 2], Xiaojiao Hu[1, 2], Yujin Wu[1, 2], Qi Wang[1, 2], Feiqian Ma[1, 2], Shuqiang Li[1], Hongwu Wang[1, 2, *], Zhifang Liu[1, 2, *]& Changling Huang[1, 2, *]

[1] Institute of Crop Sciences, Chinese Academy of Agricultural Sciences, Beijing, China.

[2] National Engineering Laboratory for Crop Molecular Breeding, Beijing, China.

#Equal contributors

Correspondence:

*Hongwu Wang

wanghongwu@caas.cn

*Zhifang Liu

liuzhifang@caas.cn

*Changling Huang

huangchangling@caas.cn

Abstract

Background

Cell wall architecture plays a key role in stalk strength and forage digestibility. Lignin, cellulose and hemicellulose are the three main components of the plant cell wall and can impact stalk quality by affecting cell wall structure and strength. To explore cell wall development during secondary cell wall lignification in maize stalks, conventional and conditional genetic mappings was used to identify the dynamic quantitative trait locus (QTL) for cell wall components and digestibility traits in five growth stages after silking.

Results

Acid detergent lignin (ADL), cellulose (CEL), Acid detergent fiber (ADF), neutral detergent fiber (NDF), and *in vitro* dry matter digestibility (IVDMD) of stalk were evaluated in a maize recombinant inbred line (RIL) population. The cell wall components gradually increased in the 10–40 days after silking (DAS), reached a maximum at 30–40 DAS, and then steadily decreased. IVDMD decreased over the initial 40 DAS and then increased slightly. Seventy-two QTL were identified for five traits and each accounted for 3.48-24.04% of the phenotypic resistance variation. Twenty-six conditional QTL were detected using conditional QTL mapping. 22 out of 24 conditional QTL were found for stages III|II and V|IV. Six QTL hotspots were found localized in bins 1.08, 2.04, 2.07, 7.03, 8.05, and 9.03 in the maize genome.

Conclusion

The unconditional pleiotropic QTL in bins 1.08 and 8.05 were also associated with stalk strength. Furthermore, several pleiotropic QTL for cell wall and digestibility were

found not associated with stalk strength. A simultaneous improvement in forage digestibility and lodging resistance can be achieved by pyramiding multiple effective QTL identified in the present study.

Keywords: Quantitative trait locus, Maize (*Zea mays* L.), Cell Wall Components, Forage quality.

Background

Maize (*Zea mays* L.) can be bio-refined to provide sustainable bioproducts and bioenergy [1]. More importantly, the stover of this staple crop is usually treated as a significant feed resource for ruminant animal production in China. The cell walls of maize plants not only provide mechanical tissues for structure support and protection but also determine feeding value by affecting forage digestibility. Plant cell walls consist of cellulose, which is Earth's most abundant organic compound; lignin, the world's most abundant resource of bio-aromatics; and hemicelluloses (xylan and glucomannan) [2]. Lignin contributes the most to resistance to digestion [3]. Lignin has a variable decreasing effect on degradation because of changes in content in the cell wall, its variable structure, and how it binds to other cell wall components [4]. Given that the forage quality is a complex and integrated trait that can be affected by many factors, breeders are inclined to improve forage quality by using integrated or digestibility traits, such as NDF, ADF, and IVDMD.

In addition to the efforts made to improve the forage quality of silage maize, several studies were performed to dissect the genetic architecture of forage digestibility and related traits. With the development of molecular biology and genetics, researchers are eager to know the genetic correlation between cell wall components and forage digestibility and mine elite resources and genes to improve the digestibility of silage maize. As an alternative strategy, mutants that induce high cell wall digestibility can be

used in silage maize breeding for feeding value; mutants are also ideal genetic material for mining genes that codify cell wall biosynthesis. Brown midrib (*bm*) mutant plants accumulate reddish-brown pigmentation in the leaf midrib and stalk. These mutants have significantly reduced lignin content and/or high cell wall digestibility [5]. To date, six *bm* mutants have been identified in maize. The *bm1*, *bm* 2, *bm*3, and *bm*4 loci encode cinnamyl alcohol dehydrogenase, methylenetetrahydrofolate reductase, caffeic acid *O*-methyltransferase, and folylpolyglutamate synthase, respectively [6-10]. These genes are associated with lignin biosynthesis and the upstream monolignol pathway. Furthermore, the *bm5* mutation has been mapped in bin 5.04 and encode 4-coumarate: coenzyme A ligase [11, 12]. By fine mapping, *bm6* was finally mapped to a 180 kb region on chromosome 2 [13].

Because of its excellent performance in increasing silage intake and milk production, the *bm3* mutant has been widely used in cell wall digestibility and feeding value improvements in commercial hybrids. Comparisons of normal and *bm3* silage hybrids have revealed the powerful effect of *bm3* on improving feeding value and cell wall digestibility [14]. However, *bm* mutants are associated with a reduction in dry matter yield and changes in days to flowering [15], as well as stress tolerance including lodging, drought, pest, and disease [14]. Therefore, one of the key strategies to improve silage maize with *bm* mutants is to find the appropriate balance between feeding value and agronomic traits.

In addition to mutant utilization in silage maize breeding, studies have been performed to dissect the genetic basis of cell wall-related traits and silage quality by using quantitative genetic approaches. Besides major mutations, QTL with small effects contribute to genetic variation of forage digestibility. Several studies have been carried out to detect QTL for cell wall composition and digestibility traits [16-29], and four hotspots of QTL were found located in bins 2.08, 5.03, 6.04, and 9.06 [30]. To summarize the QTL information, a meta-analysis was performed on the results of these

studies, and eight highlighted regions of meta-QTL for both digestibility and cell wall traits were identified [31]. The genetic variation of digestibility and cell wall-related traits are, thus, controlled by several major effect loci and numerous minor effect QTL that are distributed over the maize genome. Although numerous QTL have been identified for cell wall and digestibility related traits, few have been used in marker-assisted breeding programs. Moreover, because cell wall biosynthesis is the result of a dynamic process that consists of physiological and biochemical changes, a genetic analysis of cell wall and digestibility traits might not provide a reasonable explanation for forage quality. In this study, a maize RIL population was used to investigate the genetic relationships between cell wall compositions and digestibility traits. The objectives were to (1) identify the dynamic QTL related to cell wall composition and digestibility by using conventional and conditional mapping methods and (2) dissect the genetic basis of the cell wall components and digestibility in maize.

Materials and methods

Development of the RIL population and field experiments

An RIL population consisting of 215 lines was developed using the single seed descent method from an elite hybrid Zhongdan909. The parental lines of this commercial hybrid are Zheng58, which is one of the most commonly used parental lines in China, and HD568. All F_{10} RILs and the two parental lines were planted in 2012, in the Winter Nursery Farm of the Chinese Academy of Crop Sciences (Sanya, 109°10′E, 18°21′N), a famous winter nursery located in southern China. The genetic materials were planted in 2013 in the Agronomy Farm of the Chinese Academy of Crop Sciences (Beijing 116°34′E, 39°54′N). The field experimental design followed an incomplete block design approach, with two replications at each location. Each line was grown in a single 2.5 m row with 0.67 m between rows and a planting density of 45,000 plants/ha.

Phenotyping methods

The silking date was recorded when 50% of the silks emerged from all plants in each line. The 2nd–5th internodes above the ground from six plants of each line were collected using garden shears at 10, 20, 30, 40, and 50 DAS, respectively. All samples were immediately enzyme-deactivated at 105°C for 30 min and air-dried for 10–14 days. Dried stalk samples were ground using an automatic hammer mill herb grinder and filtered through a screen with a mesh size of 0.1 mm. Before measurements, the stalk samples were dried at 45°C for 48 h to exclude the influence of moisture. CEL, ADL, ADF, NDF, and IVDMD were estimated using near-infrared reflectance spectroscopy. The samples were scanned using a near-infrared reflectance spectrophotometer (Vector 22/N, Bruker Optik, Ettlingen, Germany). A modified partial least squares approach implemented in OPUS 6.0 Bruker software was used to fit the calibration equations. The coefficients of determination for cross-validation (R^2_{cv}) ranged from 90.2% (IVDMD) to 94.0% (CEL), and the coefficients of external validation (R^2_{val}) were 92.7% for ADL, 96.7% for CEL, 94.6% for ADF, 96.5% for NDF, and 91.2% for IVDMD.

Phenotypic data analyses

A mixed linear model implemented with the "lmer" function in the "lme4" package in R version 3.6.0 (R development Core Team, 2019) was fitted to calculate the best linear unbiased prediction (BLUP) value for each line: $y_i = \mu + g_i + e_i + \varepsilon_i$, where y_i represents the phenotype of the "i"th line, μ is the grand mean value of the target trait in all environments, g_i represents the genetic effect, e_i is the environmental effect (replications in each environment were also treated as environmental effects in the BLUP mixed model), and ε_i is the random error. The grand mean was fitted as a fixed effect, and genotype and environment were considered as random effects. The estimated BLUP was denoted as the sum of the grand mean and genetic effects of each line. The BLUP values of each line were used as phenotypic values for QTL mapping.

A standard analysis of variance was conducted using the base "aov" function in R. The model used for the analysis of variance was $y_{ilk} = \mu + e_l + r_{k(l)} + f_i + (fe)_{il} + \varepsilon_{ilk}$, where e_l is the environmental effect of the "l"th environment, $r_{k(l)}$ is the effect of replications within environments, f_i represents the genetic effect of the "i"th line, $(fe)_{il}$ is the interaction effect between genetic and environment effects, and ε_{ilk} is the residual error. All the effects were considered as random effects. Broad-sense heritability was calculated as $H^2 = \sigma_g^2/(\sigma_g^2 + \sigma_{ge}^2/e + \sigma_\varepsilon^2/re)$, where σ_g^2 represents the genetic variance, σ_{ge}^2 is the variance of interaction between the genotype and environment, σ_ε^2 is the residual error variance item, and e and r are the number of environments and replications in each environment, respectively. The 95% confidence intervals of H^2 were calculated following the method of Knapp et al. [32].

Genotyping and genetic map construction

Leaf tissues were collected from all 215 RILs and their parental lines and freeze-dried at -60°C. Genomic DNA was extracted using the modified CTAB method [33] and used for genotyping with the maize 55K single-nucleotide polymorphism (SNP) array [34]. The quality of each SNP was manually controlled as described by Yan et al. [35], and SNPs with poor quality were excluded from further analysis. PLINK [36] was used to estimate the minor allele frequency (MAF), missing rate, and heterozygosity for each SNP, as well as the missing rate and heterozygosity for each line. After quality control, SNPs with a missing rate ≤ 20%, heterozygosity ≤ 10%, and MAFs ≥ 0.05 were used to construct the genetic linkage map; 14,544 SNPs were used in constructing the genetic map for the RIL population. Finally, the genetic bin map of 1519.5 cM was constructed using ASMap for R [37], and map distances were calculated using the Kosambi mapping function [38].

QTL mapping

BLUP values across environments were used in QTL mapping of the cell wall

components and digestibility traits. A whole-genome scan was performed using composite interval mapping (*cim*) implemented in the R package *R/qtl* (version 1.44-9) [39]. A test with 1,000 permutations was performed to generate the logarithm of odds (LOD) significance threshold, which was set at $\alpha < 0.05$ [40]. The confidence intervals for the locations of the QTL were determined via 1.5-LOD support intervals to each side of the position of the maximum LOD.

In addition to the unconditional QTL mapping, dynamic conditional QTL mapping was performed using the composite interval mapping method. Conditional phenotypic values were the cell wall component trait values in adjacent stages, which represent the extra genetic effect, ΔG, between the genetic effect at stage *t* ($G_{(t)}$) and that at stage t-1 ($G_{(t-1)}$). The conditional phenotypic values $y_{(t|t-1)}$ were obtained by the mixed model implemented in QGAStation 2.0 (http://ibi.zju.edu.cn/software/qga/) [41] and were subsequently treated as unconditional phenotypic values to perform composite interval mapping with the R/qtl package.

Results

Phenotypic variation and correlation between traits

Each line of the RIL population was sampled at five stages, including 10–50 DAS (denoted as stages I, II, III, IV, and V), and evaluated for CEL, ADL, ADF, NDF, and IVDMD. For convenience, the phenotypic value of each trait at each stage was denoted as "Trait_Stage." For example, "ADF_I" represents the ADF measured at stage I. The cell wall components and digestibility traits were evaluated in five stages and two environments in the present study. The phenotypic values of ADF, NDF, CEL, and ADL in Zheng58 were slightly lower than those in HD568 at stage I, nearly equal to those in HD568 at stage II, and surprisingly surpassed those in HD568 at stages III and IV. At the final stage, the values of these traits in Zheng58 showed a significant decrease, and they were lower than those in HD568. For the RIL population, the average IVDMD

decreased over the initial four sampling stages and then increased slightly. The other four traits displayed a completely opposite tendency (Figure 1). The variation of each trait at various stages ranged from 1.21- (NDF_V) to 1.94-fold (IVDMD_IV). Meanwhile, the variation of each trait increased over the first four stages and decreased in the last stage (Figure 1). IVDMD, which ranged from -0.61 to -0.96, was negatively correlated with the other four traits in each corresponding stage. In addition, the ADF, NDF, CEL, and ADL showed high and positive correlations with each other across all stages (Figure 2). The results of the variance analysis showed that the cell wall components and digestibility of the maize stem were significantly affected by the genotype, environment, and interactions between the genotype and environment. The broad-sense heritability of the traits ranged from 0.47 (IVDMD_V) to 0.72 (ADF_I) (Table 1).

Unconditional QTL mapping

After 1,000 permutation tests, the empirical threshold LOD values for the genome-wide significance ($p < 0.05$) were determined, ranging from 3.8 to 4.1 for various stages and traits. A total of 72 unconditionally detected QTL for cell wall components and digestibility traits at five sampling stages were identified on nine chromosomes. The percentage of trait variation explained by each QTL ranged from 3.48% to 24.04%. Approximately 22.2% (16/72) QTL accounted for more than 10% of the phenotypic variation.

For ADF, 14 QTL were detected on chromosomes 1, 2, 4, 7, 8, and 9 at the five stages, individually explaining 5.20–13.48% of the phenotypic variance (Table 2). Among these QTL, two major effect QTL were detected on chromosomes 2 and 9. On chromosome 1, a QTL located at 201.5–207.8 cM was detected at multiple stages (stages I, II, and IV) and was responsible for 6.67%, 7.01%, and 6.25% of the phenotypic variance, respectively. Additionally, another consensus QTL located at 90.7–92.8 cM on chromosome 2 was found to be responsible for 13.48%, 12.13%, and

5.56% of the phenotypic variance at stages I, II, and III, respectively. Moreover, two overlapping QTL were detected at 62–66 cM and 42–45 cM on chromosomes 7 and 9, respectively.

For NDF, 16 QTL were detected on chromosomes 1, 2, 7, 8, and 9. Each QTL could explain 3.48–13.97% of the total phenotypic variance at different stages. Thirteen of the NDF-related QTL overlapped and formed four consensus QTL clusters. These hotspot loci were distributed at 202.7–20.35 cM on chromosome 1, 90.6–92.8 cM on chromosome 2, 65.3–71.4 cM on chromosome 7, and 43.1–45.2 cM on chromosome 9.

Twelve unconditional QTL for ADL were identified during the five development stages. Among these, 11 QTL were distributed on chromosomes 1, 2, and 6. Similar to that for ADF, the QTL located at 201.3–207.8 cM on chromosome 1 were identified for ADL at stages I and II. During stages I, II, and V, two consensus QTL related to ADL were found at 140.7–141.2 cM on chromosome 2 and 20.7–21.3 cM on chromosome 6. Moreover, the overlapped QTL on chromosome 2 contributed to 24.04%, 15.18%, and 16.11% of the phenotypic variance at stages I, II, and V, respectively, which seems to be a stable and major effect QTL for ADL.

During the five stages, 11 unconditional QTL for CEL were detected. These QTL were distributed on chromosomes 1, 2, 6, and 7 (Table 2, Figure 3). Each QTL could explain 5.12–18.97% of the total variance. The QTL located at 91.1–92.8 cM on chromosome 2 was repeatedly detected at stages I, II, III, and IV and contributed to 5.42–18.97% of the total phenotypic variance.

For IVDMD, 19 QTL were detected on eight chromosomes. Among these, 12 overlapping QTL were integrated into four consensus QTL. Among these overlapping QTL, four were identified repeatedly at 202.7–207.8 cM on chromosome 1. These QTL contributed to 6.66%, 12.99%, 6.76%, and 5.81% of the total phenotypic variance at stages II, III, IV, and V, respectively. In addition, the QTL located at approximately 92.0–92.8 cM on chromosome 2 was correlated with IVDMD at stages I, II, and III. On chromosome 9, the QTL at 43.1–46.0 cM was identified to be strongly related to

IVDMD at stages I, II, and V. Moreover, another overlapping QTL for IVDMD was detected on chromosome 10, which was located at 49.5–50.2 cM and contributed to 5.07% and 8.16% of the total phenotypic variance at stages I and V, respectively.

Conditional QTL mapping

In total, 26 conditional QTL were identified at five stages for cell wall components and digestibility traits (Table 3). Each QTL could explain 1.02–14.95% of the phenotypic variance. All the conditional QTL were detected on eight chromosomes, except for chromosomes 4 and 8. Approximately 61.5% (16/26) QTL were distributed on chromosomes 1 and 2.

Five ADF-related conditional QTL were identified as distributed on chromosomes 1, 2, 3, and 6. When the ADF at stage V was conditioned on the ADF at stage IV, *conqADF1b* and *conqADF2* were detected on chromosomes 1 and 2; these QTL were responsible for 10.15% and 11.99% of the total variance, respectively. At the IV|III stage, *conqADF1a* and *conqADF3* were found to contribute to 1.02% and 3.89% of the total variance, respectively. On chromosome 6, *conqADF6* was detected with a contribution of 5.40% when the ADF at stage III was conditioned on the ADF at stage II.

Four conditional QTL for ADL were detected on chromosomes 1, 2, and 10. QTL *conqADL1a* and *conqADL1b* overlapped the QTL located on chromosome 1 and contributed to 5.34% and 7.98% of the total variance for ADL at the IV|III and V|IV stages, respectively. In addition to that on chromosome 1, a conditional QTL on chromosome 2, *conqADL2*, was detected when the ADL at stage V was conditioned on the ADL at stage IV. This major effect QTL could explain 13.41% of the total variance. Moreover, at stage III|II, *conqADL10* was identified to be responsible for 4.84% of the total variance.

For CEL, five conditional QTL were found at stages III|II, IV|III, and V|IV. At stages IV|III and V|IV, QTL *conqCEL1a* and *conqCEL1b* were located at adjacent

positions on chromosome 1 and contributed to 3.93% and 10.70% to the total variance, respectively. Another major conditional QTL at the V|IV stage located on chromosome 2 was *conqCEL2* and contributed to 14.95% of the total variance. When the CEL at stage III was conditioned on the CEL at stage II, *conqCEL5* and *conqCEL7* were identified on chromosomes 5 and 7.

Conditional QTL mapping for IVDMD revealed six QTL on chromosomes 1, 2, 6, 9, and 10. These conditional QTL were identified at the III|II and V|IV stages. When the IVDMD at stage III was conditioned on the IVDMD at stage II, QTL *conqIVDMD1a*, *conqIVDMD2*, and *conqIVDMD6* were responsible for 6.39%, 6.06%, and 5.21% of the total variance, respectively. In addition, QTL *conqIVDMD1b*, *conqIVDMD9*, and *conqIVDMD10* identified at stage V|IV, could explain 8.68%, 9.08%, and 7.67% of the total variance in the IVDMD.

Similar to that for the IVDMD, six conditional QTL were identified for NDF. All these QTL were also found at stages III|II and V|IV. Moreover, three conditional QTL for NDF detected at stage III|II overlapped with the conditional QTL for IVDMD detected at the same stage (*conqIVDMD1a*, *conqIVDMD2*, and *conqIVDMD6*). At stage V|IV, three conditional QTL *conqNDF1b*, *conqNDF2b*, and *conqNDF9* contributed to 9.00%, 6.91%, and 10.12% of the total variance in the NDF. *conqNDF1b* was found to be overlapped with *conqIVDMD1b,* which was identified at stage V|IV for IVDMD.

Discussion

The area of maize in China has been expanding annually. The livestock industry requires large amounts of silage maize owing to the increase in demand for meat and milk. However, common maize is still the main variety promoted in China because of the policy of self-sufficiency in food production. Although silage maize has a large amount of biomass, higher than that of common maize, its starch and dry matter content is lower than that of common maize. Therefore, silage made of grain and forage maize

varieties is more popular in China. The critical issue is that the choice of harvesting time is a trade-off among yield, feeding value, and silage quality.

Lodging is a critical phenomenon for maize production, causing severe yield reduction during the reproductive stage. Stronger cell walls can provide more powerful mechanical support to avoid lodging. By contrast, cell wall digestibility, which is strongly affected by cell wall lignification, is a vital characteristic for the nutritional value of forage maize [42]. Cell wall lignification is a dynamic and complex process that occurs throughout maize growth. In the present study, we used a maize RIL population to investigate the dynamic changes in cell wall component and digestibility traits at five stages from silking to harvest. For each trait, no apparent differences were observed among the beginning stages. ADF, NDF, ADL, and CEL showed a massive increase at stages III and IV and exhibited a slight decrease at stage V. Conversely, IVDMD showed a large decrease at stages III and IV and exhibited a small increase at stage V. This inverse trend may be associated with significant negative correlations between these traits and IVDMD. These results revealed that the optimal harvest time for grain-forage maize was approximately 50 DAS. At this time, the plant has reached physiological maturity and the grain is in full dent stage. After harvesting for grain, the plant can also be harvested for forage or stover to feed animals. Alternatively, forage maize could be harvested between stages II and III, which is roughly in the dough stage. During this period, starch has just begun accumulating in the grains, and plant digestibility decreases slightly. Forage harvested at this stage can provide sufficient nutritional value and ensure silage quality.

Cell wall components mainly consist of cellulose, lignin, and hemicellulose. NDF mainly consists of cellulose, hemicelluloses, lignin, and some mineral substances present in the cell wall [25]. After hemicelluloses are solubilized by acid detergent treatment, the residual cellulose and lignin are left as the main part of ADF [31]. In maize, previous studies on cell wall components and digestibility traits have focused on specific stages [16, 20, 22-27, 29, 30, 43, 44], such as 10–14 DAS and the silage

harvest stage (approximately 30–35% of dry matter). QTL detected at these specific stages may not reflect the genetic effects of crop development. In the present study, to better understand the developmental characteristics of cell-wall components, we performed dynamic QTL analysis during five developmental stages after silking.

As there was no significant difference among the phenotypic values of stages I and II, no conditional QTL was found for any of the traits when stage II was conditioned on stage I. Moreover, several overlapping unconditional QTL were detected between these two stages. In general, unconditional QTL hotspots were located on chromosomes 1, 2, 7, 8, and 9. The co-localized QTL on chromosome 1 was located in bin 1.08, which corresponded to the 215–250 Mb physical region in the maize genome (Version 5.60) [45]. This genomic region was also detected as a meta-QTL hotspot for cell wall content and digestibility [31]. Moreover, this locus was shown to be associated with stalk strength in another study [38] in which QTL mapping was performed for rind penetrometer resistance (RPR) using the same RIL population that was used in the present study. We found that another pleiotropic QTL for RPR was associated with ADF, NDF, and IVDMD. This pleiotropic QTL was localized in bin 8.05 and explained 6.61–14.06% of the phenotypic variance for each trait. Therefore, this major effect QTL should be the target for fine mapping and gene cloning.

In addition to the pleiotropic QTL mentioned above, we detected several pleiotropic QTL for cell wall and digestibility; however, these were not associated with RPR. On chromosome 2, a co-localized QTL in bin 2.07 was found to be related to CEL and ADL at various stages. Another overlapped QTL in bin 2.04 was repeatedly detected for all four traits except ADL. Thus, we concluded that a cellulose synthesis gene is responsible for the genetic variation at this locus. Another overlapping QTL region was found on chromosome 7. At stage III, this QTL located in bin 7.03 was detected for all five traits. A hotspot QTL on chromosome 9 was associated with ADF, NDF, and IVDMD, which means that this QTL may affect plant digestibility by affecting cell wall components other than cellulose and lignin. All these cell wall and

digestibility QTL hotspots should be the focus of attention for further cloning of candidate genes and favorable alleles. The genes underlying these QTL should be responsible for secondary cell wall digestibility but not affect cell wall rigidity. In this context, it is possible to improve the digestibility of silage through molecular marker-assisted modification of these QTL without reducing stalk strength. Furthermore, a simultaneous improvement in forage digestibility and lodging resistance can be achieved by pyramiding multiple effective genes underlying all the pleiotropic QTL.

Most conditional QTL were mainly detected for stages III|II and V|IV owing to the significant phenotypic differences between the two adjacent stages. Six out of 26 conditional QTL explained more than 10% of the phenotypic variation for each trait. Compared with the results of unconditional mapping, conditional mapping revealed a few novel QTL. Remarkably, the genomic region in bin 1.02 was related to five traits under conditional stages and was responsible for 8.00–10.70% of the phenotypic variation. Comparatively, we verified that the pleiotropic QTL in bin 2.07 was consistently identified by both conditional and unconditional QTL mapping. These results revealed that the combination of genes expressed stably at different periods and the genes expressed only at specific periods lead to the dynamic development of cell wall components. Therefore, the application of multi-omics approaches in future studies will help to better understand the dynamic development of cell wall components and their genetic regulatory mechanisms.

In summary, we evaluated cell wall components and digestibility in multiple developmental stages after silking and revealed the law of dynamic changes in an RIL population. We identified 72 and 26 consensus QTL using unconditional and conditional QTL mapping, respectively. Our study highlighted six regions (localized in bins 1.08, 2.04, 2.07, 7.03, 8.05, and 9.03) that were of particular interest. Some of these showed pleiotropic effects on digestibility and stalk strength in maize, whereas the others could be applied to improve forage digestibility without altering lodging resistance. These findings enhance our understanding of the genetic mechanism of

maize cell wall synthesis.

Abbreviations

ADF: Acid detergent fiber; ADL: Acid detergent lignin; BLUP: Best linear unbiased prediction; CEL: cellulose; DAS: days after silking; IVDMD: *in vitro* dry matter digestibility; LOD: Logarithm of odds; NDF: Neutral detergent fiber; MAF: minor allele frequency; QTL: Quantitative trait locus/loci; RIL: recombinant inbred line; SNP: Single nucleotide polymorphism.

Reference

1. Scholey DV, Burton EJ, Williams PEV: **The bio refinery; producing feed and fuel from grain**. *Food Chem* 2016, **197**(Pt A):937.
2. Zhong R, Cui D, Ye Z-H: **Secondary cell wall biosynthesis**. *New Phytol* 2019, **221**(4):1703-1723.
3. Argillier O, Barrière Y, Hébert Y: **Genetic variation and selection criterion for digestibility traits of forage maize**. *Euphytica* 1995, **82**(2):175-184.
4. Barrière Y, Guillet C, Goffner D, Pichon M: **Genetic variation and breeding strategies for improved cell wall digestibility in annual forage crops. A review**. *Anim Res* 2003, **52**(3):193-228.
5. Barrière Y, Ralph J, Méchin V, Guillaumie S, Grabber JH, Argillier O, Chabbert B, Lapierre C: **Genetic and molecular basis of grass cell wall biosynthesis and degradability. II. Lessons from brown-midrib mutants**. *C R Biol* 2004, **327**(9-10):847-860.
6. Vignols F, Rigau J, Torres MA, Capellades M, Puigdomènech P: **The brown midrib3 (bm3) mutation in maize occurs in the gene encoding caffeic acid O-methyltransferase**. *Plant Cell* 1995, **7**(4):407-416.
7. Chen W, VanOpdorp N, Fitzl D, Tewari J, Friedemann P, Greene T, Thompson S, Kumpatla S, Zheng P: **Transposon insertion in a cinnamyl alcohol dehydrogenase gene is responsible for a brown midrib1 mutation in maize**. *Plant Mol Biol* 2012, **80**(3):289-297.
8. Tang HM, Liu S, Hill-Skinner S, Wu W, Reed D, Yeh CT, Nettleton D, Schnable PS: **The maize brown midrib2 (bm2) gene encodes a methylenetetrahydrofolate reductase that contributes to lignin accumulation**. *Plant J* 2014, **77**(3):380-392.
9. Li L, Hill-Skinner S, Liu S, Beuchle D, Tang HM, Yeh CT, Nettleton D, Schnable PS: **The maize brown midrib4 (bm4) gene encodes a functional folylpolyglutamate synthase**. *Plant J* 2015, **81**(3):493-504.
10. Halpin C, Holt K, Chojecki J, Oliver D, Chabbert B, Monties B, Edwards K, Barakate A, Foxon GA: **Brown‐midrib maize (bm1)–a mutation affecting the cinnamyl alcohol dehydrogenase gene**.

Plant J 1998, **14**(5):545-553.

11. Haney L, Hake S, Scott M: **Allelism testing of Maize Coop Stock Center lines containing unknown brown midrib alleles**. *Maize Genetics Cooperative Newsletter* 2008, **82**.
12. Xiong W, Wu Z, Liu Y, Li Y, Su K, Bai Z, Guo S, Hu Z, Zhang Z, Bao Y *et al*: **Mutation of 4-coumarate: coenzyme A ligase 1 gene affects lignin biosynthesis and increases the cell wall digestibility in maize brown midrib5 mutants**. *Biotechnol Biofuels* 2019, **12**:82.
13. Chen Y, Liu H, Ali F, Scott MP, Ji Q, Frei UK, Lubberstedt T: **Genetic and physical fine mapping of the novel brown midrib gene bm6 in maize (Zea mays L.) to a 180 kb region on chromosome 2**. *Theor Appl Genet* 2012, **125**(6):1223-1235.
14. Barrière Y: **Brown-midrib genes in maize and their efficiency in dairy cow feeding. Perspectives for breeding improved silage maize targeting gene modifications in the monolignol and p-hydroxycinnamate pathways**. *Maydica* 2017, **62**(2017):M21.
15. Vermerris W, Mcintyre LM: **Time to flowering in brown midrib mutants of maize: an alternative approach to the analysis of developmental traits**. *Heredity* 2010, **83**(2):171-178.
16. Lübberstedt T, Melchinger AE, Klein D, Degenhardt H, Paul C: **QTL mapping in testcrosses of European flint lines of maize: II. Comparison of different testers for forage quality traits**. *Crop Sci* 1997, **37**(6):1913-1922.
17. Lübberstedt T, Melchinger AE, Schön CC, Utz HF, Klein D: **QTL mapping in testcrosses of European flint lines of maize: I. Comparison of different testers for forage yield traits**. *Crop Sci* 1997, **37**(3):921-931.
18. Bohn M, Schulz B, Kreps R, Klein D, Melchinger A: **QTL mapping for resistance against the European corn borer (Ostrinia nubilalis H.) in early maturing European dent germplasm**. *Theor Appl Genet* 2000, **101**(5-6):907-917.
19. Barriere Y, Gibelin C, Argillier O, Mechin V: **Genetic analysis in recombinant inbred lines of early dent forage maize. I: QTL mapping for yield, earliness, starch and crude protein contents from per se value and top cross experiments**. *Maydica* 2001, **46**(4):253-266.
20. Méchin V, Argillier O, Hébert Y, Guingo E, Moreau L, Charcosset A, Barrière Y: **Genetic analysis and QTL mapping of cell wall digestibility and lignification in silage maize**. *Crop Sci* 2001, **41**(3):690-697.
21. Papst C, Melchinger A, Eder J, Schulz B, Klein D, Bohn M: **QTL mapping for resistance to European corn borer (Ostrinia nubilalis Hb.) in early maturing European dent maize (Zea mays L.) germplasm and comparison of genomic regions for resistance across two populations of F3 families**. *Maydica* 2001, **46**(3):195-205.
22. Roussel V, Gibelin C, Fontaine A, Barriere Y: **Genetic analysis in recombinant inbred lines of early dent forage maize. II. QTL mapping for cell wall constituents and cell wall digestibility from per se value and top cross experiments**. *Maydica* 2002, **47**(1):9-20.
23. Cardinal AJ, Lee M, Moore KJ: **Genetic mapping and analysis of quantitative trait loci affecting fiber and lignin content in maize**. *Theor Appl Genet* 2003, **106**(5):866-874.
24. Fontaine A, Briand M, Barriere Y: **Genetic variation and QTL mapping of para-coumaric and ferulic acid**. *Maydica* 2003, **48**:75-84.
25. Krakowsky M, Lee M, Beeghly H, Coors J: **Characterization of quantitative trait loci affecting fiber and lignin in maize (Zea mays L.)**. *Maydica* 2003, **48**(4):283-292.

26. Krakowsky MD, Lee M, Coors JG: **Quantitative trait loci for cell-wall components in recombinant inbred lines of maize (*Zea mays* L.) I: stalk tissue**. *Theor Appl Genet* 2005, **111**(2):337-346.
27. Krakowsky MD, Lee M, Coors JG: **Quantitative trait loci for cell wall components in recombinant inbred lines of maize (*Zea mays* L.) II: leaf sheath tissue**. *Theor Appl Genet* 2006, **112**(4):717-726.
28. Barrière Y, Riboulet C, Méchin V, Maltese S, Pichon M, Cardinal A, Lapierre C, Lubberstedt T, Martinant J-P: **Genetics and genomics of lignification in grass cell walls based on maize as model species**. *Genes Genomes Genomics* 2007, **1**:133-156.
29. Riboulet C, Fabre F, Dénoue D, Martinant J, Lefevre B, Barrière Y: **QTL mapping and candidate gene research from lignin content and cell wall digestibility in a top-cross of a flint maize recombinant inbred line progeny harvested at silage stage**. *Maydica* 2008, **53**(1):1.
30. Barrière Y, Thomas J, Denoue D: **QTL mapping for lignin content, lignin monomeric composition, p-hydroxycinnamate content, and cell wall digestibility in the maize recombinant inbred line progeny F838×F286**. *Plant Sci* 2008, **175**(4):585-595.
31. Truntzler M, Barriere Y, Sawkins MC, Lespinasse D, Betran J, Charcosset A, Moreau L: **Meta-analysis of QTL involved in silage quality of maize and comparison with the position of candidate genes**. *Theor Appl Genet* 2010, **121**(8):1465-1482.
32. Knapp S, Stroup W, Ross W: **Exact confidence intervals for heritability on a progeny mean basis**. *Crop Sci* 1985, **25**(1):192-194.
33. Murray MG, Wf. T: **Rapid isolation of high molecular weight plant DNA**. *Nucleic Acids Res* 1980, **8**(19):4321-4325.
34. Xu C, Ren Y, Jian Y, Guo Z, Zhang Y, Xie C, Fu J, Wang H, Wang G, Xu Y: **Development of a maize 55 K SNP array with improved genome coverage for molecular breeding**. *Mol Breeding* 2017, **37**(3):1-12.
35. Yan J, Yang X, Shah T, Sánchez-Villeda H, Li J, Warburton M, Yi Z, Crouch JH, Xu Y: **High-throughput SNP genotyping with the GoldenGate assay in maize**. *Mol Breeding* 2010, **25**(3):441-451.
36. Purcell S, Neale B, Toddbrown K, Thomas L, Ferreira MAR, Bender D, Maller J, Sklar P, Bakker PIWD, Daly MJ: **PLINK: A tool set for whole-genome association and population-based linkage analyses**. *Am J Hum Genet* 2007, **81**(3):559-575.
37. Taylor J, Butler D: **R Package ASMap: Efficient Genetic Linkage Map Construction and Diagnosis**. *Journal of Statistical Software* 2017, **079**(6).
38. Liu X, Hu X, Li K, Liu Z, Wu Y, Wang H, Huang C: **Genetic mapping and genomic selection for maize stalk strength**. *BMC Plant Biol* 2020, **20**(1):196.
39. Arends D, Prins P, Jansen RC, Broman KW: **R/qtl: high-throughput multiple QTL mapping**. *Bioinformatics* 2010, **26**(23):2990-2992.
40. Churchill GA, Doerge RW: **Empirical threshold values for quantitative trait mapping**. *Genetics* 1994, **138**(3):963-971.
41. Zhu J: **Analysis of conditional genetic effects and variance components in developmental genetics**. *Genetics* 1995, **141**(4):1633-1639.
42. Mechin V, Argillier O, Menanteau V, Barriere Y, Mila I, Pollet B, Lapierre C: **Relationship of cell**

wall composition to in vitro cell wall digestibility of maize inbred line stems. *Journal of the Science of Food & Agriculture* 2000, **80**(5):574–580.

43. Lübberstedt T, Melchinger AE, Fähr S, Klein D, Dally A, Westhoff P: **QTL mapping in testcrosses of flint lines of maize: III. Comparison across populations for forage traits**. *Crop Sci* 1998, **38**(5):1278-1289.

44. Barrière Y, Méchin V, Denoue D, Bauland C, Laborde J: **QTL for yield, earliness, and cell wall quality traits in topcross experiments of the F838× F286 early maize RIL progeny**. *Crop Sci* 2010, **50**(5):1761-1772.

45. **MaizeSequence** [http://ensembl.gramene.org/Zea_mays/Info/Index]

Declarations

Ethics approval and consent to participate

Not applicable

Consent for publication

Not applicable

Availability of data and material

The datasets supporting the conclusions of this article are included within the article and its additional files.

Competing interests

The authors declare that they have no competing interests.

Funding

This research was supported by the National Key Research and Development Program of China (Grant No. 2016YFD0101200), the National Natural Science Foundation of China (Grant No. 31801367), and the Agricultural Science and Technology Innovation Program at CAAS.

Authors' contributions

XY carried out the experiments and analyzed the data, KL analyzed the data and wrote the manuscript; XL constructed a genetic map for QTL mapping; XH, FM, QW, YW, and SL assisted in data collection and field experiment; ZL and HW constructed the RIL population and helped revise the manuscript; ZL, HW, and CH conceived and designed the study. All authors have read and approved this manuscript.

Acknowledgements

not applicable

Figures

Figure 1. Changes in cell wall components and digestibility traits after silking in a recombinant inbred line (RIL) population. ADF, acid detergent fiber; ADL, acid detergent lignin; CEL, cellulose; NDF, neutral detergent fiber; IVDMD, in vitro dry matter digestibility. I–V represent 10–50 days after silking, respectively.

Figure 2. Correlation coefficients among acid detergent fiber (ADF), neutral detergent fiber (NDF), cellulose (CEL), acid detergent lignin (ADL), and in vitro dry matter digestibility (IVDMD) across five stages.

Figure 3. Chromosomal locations of quantitative trail loci (QTL) for cell wall components and digestibility traits in a maize recombinant inbred line (RIL) population.

Tables

Table 1. Phenotypic values of cell wall components and digestibility traits at different developmental stages in a maize recombinant inbred line (RIL) population

Trait	Type		Stage				
			I	II	III	IV	V
ADF	Zheng58	Mean	24.46	24.86	32.67	40.96	30.89
	HD568	Mean	27.49	23.58	29.15	35.29	33.16
	RIL	Mean ± SD	35.34 ± 2.45	34.73 ± 2.78	38.94 ± 5.30	43.69 ± 5.16	43.16 ± 1.72
		Range	27.90–41.86	26.63–44.14	28.57–54.76	32.02–55.70	37.96–48.77
		H^2	0.72	0.56	0.64	0.59	0.49
CEL	Zheng58	Mean	21.3	22.93	29.2	36.98	28.17
	HD568	Mean	23.5	21.82	25.97	33.13	29.3
	RIL	Mean ± SD	25.07 ± 1.87	25.16 ± 1.91	27.61 ± 3.04	30.11 ± 2.57	29.3 ± 1.35
		Range	19.53–28.64	19.72–31.33	19.82–36.02	22.38–36.52	25.13–33.26
		H^2	0.72	0.56	0.61	0.49	0.52
IVDMD	Zheng58	Mean	71.68	71.2	52.87	33.55	52.88
	HD568	Mean	63.63	71.23	63.75	46.47	46.26
	RIL	Mean ± SD	59.56 ± 3.43	58.70 ± 3.55	52.63 ± 6.92	47.49 ± 6.90	50.27 ± 2.61
		Range	49.40–69.90	47.52–66.42	34.52–66.98	32.74–63.64	41.97–57.54
		H^2	0.63	0.52	0.67	0.62	0.47
ADL	Zheng58	Mean	6.47	6.85	7.64	8.57	7.62
	HD568	Mean	7.02	6.56	7.72	8.32	7.54

		Mean ± SD	7.50 ± 0.38	7.58 ± 0.41	7.75 ± 0.54	8.16 ± 0.51	8.00 ± 0.28
	RIL	Range	5.93–8.35	6.46–8.70	6.23–9.27	6.82–9.43	7.03–8.84
		H^2	0.78	0.56	0.66	0.62	0.55
	Zheng58	Mean	49.85	48.37	59.93	70.93	54.94
	HD568	Mean	52.36	48.53	53.13	60.58	57.54
NDF		Mean ± SD	51.78 ± 3.22	51.18 ± 3.32	56.88 ± 6.47	62.00 ± 6.49	61.98 ± 2.11
	RIL	Range	43.37–60.55	41.84–62.88	44.87–76.85	47.6–76.96	56.69–68.62
		H^2	0.68	0.48	0.64	0.56	0.48

553 H^2 Broad-sense heritability.

554

555 **Table 2. Unconditional consensus quantitative trail loci (QTL) underlying cell wall components and digestibility traits at different stages**

QTL	Chr[a]	Bin	Peak[b]	The closest marker	CI[c]	LOD	PVE[d]	Add.[e]
ADF_I_1	1	1.08	201.54	lmk297	198.74–206.06	4.30	6.67	0.64
ADF_I_2	2	2.04	90.56	lmk522	85.63–94.68	8.96	13.48	-0.91
ADF_I_7	7	7.03	66.66	lmk1667	62.88–70.94	5.24	6.16	0.62
ADF_I_9	9	9.03	42.56	lmk1992	40.7–47.16	9.09	10.57	0.81
ADF_II_1	1	1.08	202.65	lmk299	200.49–206.06	5.89	7.01	0.73
ADF_II_2	2	2.04	91.12	lmk523	85.63–94.68	7.52	12.13	-0.97
ADF_II_8	8	8.05	63.19	lmk1844	58.77–66.23	5.15	6.61	0.72
ADF_III_2	2	2.04	92.83	lmk525	89.26–96.56	5.56	5.45	-1.24
ADF_III_7	7	7.03	62.64	lmk1661	58.97–66.66	4.95	5.70	1.27
ADF_IV_1	1	1.08	207.82	lmk309	203.91–211.34	5.92	6.26	1.29
ADF_IV_4	4	4.03	12.30	lmk981	8.45–17.95	4.03	5.20	1.18
ADF_V_1	1	1.03	59.45	lmk80	58.41–66.45	4.18	6.69	0.44
ADF_V_2	2	2.07	138.80	lmk588	134.51–143.69	6.60	8.45	-0.51
ADF_V_9	9	9.03	45.24	lmk1999	40.7–49.86	4.30	8.04	0.49
ADL_I_1	1	1.08	201.33	lmk296	200.49–207.16	6.62	7.70	0.11
ADL_I_2	2	2.07	140.76	lmk593	137.14–143.69	16.73	24.04	-0.19
ADL_I_6	6	6.01	20.68	lmk1431	17.85–21.34	5.49	7.23	0.10
ADL_II_1	1	1.09	229.47	lmk338	225.93–233.4	5.31	6.88	0.11
ADL_II_2	2	2.07	141.24	lmk594	139.07–143.69	8.99	15.18	-0.16
ADL_II_6	6	6.01	20.68	lmk1431	17.85–22.57	5.54	8.68	0.12
ADL_III_2	2	2.04	83.60	lmk514	80.7–87.83	7.04	7.13	-0.14

ADL_III_6	6	6.01	14.47	lmk1419	11.52–17.85	5.81	7.72	0.15
ADL_III_7	7	7.03	67.52	lmk1668	63.82–70.94	4.10	4.26	0.11
ADL_IV_1	1	1.08	207.82	lmk309	204.85–214.26	4.59	6.39	0.13
ADL_V_2	2	2.07	141.24	lmk594	137.86–144.65	12.08	16.11	-0.11
ADL_V_6	6	6.01	21.34	lmk1433	19.17–25.26	5.55	7.07	0.07
CEL_I_1	1	1.09	232.92	lmk346	229.11–234.6	5.21	6.32	0.47
CEL_I_2	2	2.04	91.12	lmk523	85.63–95.63	4.94	9.21	-0.81
CEL_I_2	2	2.07	140.76	lmk593	139.07–143.69	5.45	13.82	-0.90
CEL_I_6	6	6.01	20.68	lmk1431	17.85–24.33	5.57	7.24	0.50
CEL_II_2	2	2.04	91.12	lmk523	85.63–94.68	5.34	18.97	-0.83
CEL_III_2	2	2.04	91.12	lmk523	87.83–95.63	6.03	7.52	-0.84
CEL_III_7	7	7.03	62.64	lmk1661	58.97–66.66	5.70	6.15	0.76
CEL_IV_2	2	2.04	92.83	lmk525	89.26–96.56	4.28	5.42	-0.60
CEL_V_1	1	1.03	62.79	lmk87	58.41–66.45	6.36	8.63	0.40
CEL_V_1	1	1.08	202.65	lmk299	200.49–206.06	4.22	5.12	0.21
CEL_V_2	2	2.07	136.78	lmk583	135.34–140.76	10.46	16.88	-0.56
IVDMD_I_2	2	2.04	91.96	lmk524	85.63–94.68	4.94	7.77	0.97
IVDMD_I_7	7	7.03	71.42	lmk1676	68.99–77.63	5.46	5.71	-0.82
IVDMD_I_9	9	9.03	43.07	lmk1994	40.7–46.92	11.18	13.53	-1.28
IVDMD_I_10	10	10.07	49.46	lmk2120	48.72–50.17	5.64	5.07	0.79
IVDMD_II_1	1	1.08	202.65	lmk299	200.13–206.06	6.26	6.66	-0.92
IVDMD_II_2	2	2.04	92.83	lmk525	89.26–96.56	6.16	7.13	0.97
IVDMD_II_4	4	4.05	30.98	lmk1014	26.63–34.83	4.40	4.69	-0.78
IVDMD_II_8	8	8.05	63.55	lmk1845	58.77–66.23	7.40	9.43	-1.10
IVDMD_II_9	9	9.03	44.52	lmk1997	40.7–46.92	4.48	6.35	-0.90

IVDMD_III_1	1	1.08	205.33	lmk305	201.54–209.07	8.07	12.98	-2.53
IVDMD_III_2	2	2.04	92.83	lmk525	91.12–98.23	6.35	4.55	1.48
IVDMD_III_5	5	5.02	32.93	lmk1189	28.74–39.46	4.22	5.75	1.67
IVDMD_III_7	7	7.03	62.64	lmk1661	58.97–66.66	6.01	8.11	-1.99
IVDMD_IV_1	1	1.08	207.82	lmk309	203.91–211.34	7.19	6.76	-1.79
IVDMD_V_1	1	1.08	203.45	lmk301	201.54–207.16	4.15	5.81	-0.63
IVDMD_V_2	2	2.05	106.49	lmk539	102.91–110.58	4.25	4.69	0.57
IVDMD_V_8	8	8.05	58.28	lmk1828	52.91–61.39	4.09	4.80	-0.58
IVDMD_V_9	9	9.03	45.96	lmk2000	42.83–46.92	7.33	9.33	-0.81
IVDMD_V_10	10	10.07	50.17	lmk2121	48.97–50.17	7.37	8.16	0.76
NDF_I_1	1	1.08	203.45	lmk301	201.54–206.06	5.13	5.77	0.78
NDF_I_2	2	2.04	90.56	lmk522	85.63–94.68	9.33	10.15	-1.05
NDF_I_7	7	7.03	71.42	lmk1676	68.99–75.22	5.67	5.98	0.80
NDF_I_8	8	8.01	20.24	lmk1771	17.84–23.76	4.54	6.73	0.86
NDF_I_9	9	9.03	43.07	lmk1994	40.7–46.92	9.69	12.69	1.16
NDF_II_1	1	1.08	202.65	lmk299	200.13–206.06	6.42	9.94	1.05
NDF_II_2	2	2.04	92.83	lmk525	85.63–94.68	7.99	13.97	-1.25
NDF_II_7	7	7.03	67.52	lmk1668	63.82–71.18	4.22	3.48	0.63
NDF_II_8	8	8.05	63.19	lmk1844	59.5–67.19	6.08	7.32	0.91
NDF_III_1	1	1.08	202.65	lmk299	198.13–203.2	6.96	10.65	2.12
NDF_III_2	2	2.04	91.12	lmk523	89.26–96.56	5.41	5.73	-1.56
NDF_III_7	7	7.03	65.25	lmk1665	58.97–66.66	5.54	6.63	1.68
NDF_IV_1	1	1.08	207.82	lmk309	203.91–211.34	7.34	7.10	1.72
NDF_V_1	1	1.08	202.65	lmk299	200.49–205.33	4.55	6.65	0.55
NDF_V_2	2	2.06	129.27	lmk572	126.27–132.58	5.64	7.73	-0.60

NDF_V_9	9	9.03	45.24		lmk1999	40.7–46.92	7.44	11.71	0.73

[a] Chromosome.

[b] Peak genetic position with the greatest logarithm of odds (LOD).

[c] The 1.5-LOD confidence interval (CI) of QTL.

[d] Phenotypic variation explained by the additive effects of the mapped QTL.

[e] Additive effect of the identified QTL: a positive value indicates that the Z58 allele increased trait expression, and a negative value indicates that the HD568 allele increased expression.

562 **Table 3. Conditional consensus quantitative trail loci (QTL) underlying cell wall components and digestibility traits at different stages.**

Trait	QTL	Chr[a]	Bin	Peak[b]	The closest marker	CI[c]	LOD	PVE[d]	Add[e]
ADF_III|ADF_II	conqADF6	6	6.04	37.06	lmk1458	33.02–40.98	4.94	5.40	0.86
ADF_IV|ADF_III	conqADF1a	1	1.04	103.67	lmk156	101.98–107.31	4.14	1.02	0.30
ADF_IV|ADF_III	conqADF3	3	3.03	21.8	lmk702	18.09–25.4	4.32	3.89	-0.58
ADF_V|ADF_IV	conqADF1b	1	1.02	59.45	lmk80	58.41–66.45	8.11	10.15	0.52
ADF_V|ADF_IV	conqADF2	2	2.07	138.8	lmk588	134.51–143.69	5.69	11.99	-0.56
ADL_III|ADL_II	conqADL10	10	10.06	37.16	lmk2097	33.57–41.01	4.41	4.84	0.08
ADL_IV|ADL_III	conqADL1a	1	1.02	41.59	lmk59	37.73–45.8	5.08	5.34	-0.06
ADL_V|ADL_IV	conqADL1b	1	1.02	47.25	lmk68	43.52–51.09	4.84	7.98	0.07
ADL_V|ADL_IV	conqADL2	2	2.07	143.69	lmk595	137.14–144.65	6.73	13.41	-0.09
CEL_III|CEL_II	conqCEL5	5	5.02	32.93	lmk1189	28.74–37.06	4.06	5.08	-0.49
CEL_III|CEL_II	conqCEL7	7	7.03	62.64	lmk1661	60.96–66.66	6.96	5.43	0.51
CEL_IV|CEL_III	conqCEL1a	1	1.02	41.59	lmk59	37.73–45.8	4.04	3.93	-0.32
CEL_V|CEL_IV	conqCEL1b	1	1.02	52.77	lmk74	48.15–56.5	9.25	10.70	0.41
CEL_V|CEL_IV	conqCEL2	2	2.07	136.78	lmk583	132.95–140.76	5.57	14.95	-0.49
IVDMD_III|IVDMD_II	conqIVDMD1a	1	1.10	232.92	lmk346	230.98–234.6	6.46	6.39	-1.29
IVDMD_III|IVDMD_II	conqIVDMD2	2	2.07	151.59	lmk607	146.92–155.5	5.05	6.06	-1.25
IVDMD_III|IVDMD_II	conqIVDMD6	6	6.04	43.35	lmk1462	37.06–47.26	4.43	5.21	-1.17
IVDMD_V|IVDMD_IV	conqIVDMD10	10	10.07	50.17	lmk2121	46.8–50.17	4.23	7.67	0.69
IVDMD_V|IVDMD_IV	conqIVDMD1b	1	1.02	56.5	lmk77	52.77–60.51	6.23	8.68	-0.72
IVDMD_V|IVDMD_IV	conqIVDMD9	9	9.02	28.05	lmk1957	22.26–29.74	5.61	9.08	-0.74
NDF_III|NDF_II	conqNDF1a	1	1.10	231.95	lmk342	227.68–237.83	5.42	6.24	1.16
NDF_III|NDF_II	conqNDF2a	2	2.07	151.59	lmk607	146.92–154.25	7.96	6.00	1.13
NDF_III|NDF_II	conqNDF6	6	6.04	46.06	lmk1463	43.35–51.12	4.32	5.82	1.13

NDF_V|NDF_IV	conqNDF1b	1	1.02	52.77	lmk74	50.02–56.5	7.81	8.99	0.59
NDF_V|NDF_IV	conqNDF2b	2	2.07	138.8	lmk588	134.51–143.69	5.59	6.91	-0.53
NDF_V|NDF_IV	conqNDF9	9	9.03	45.96	lmk2000	42.01–49.86	7.03	10.12	0.63

[a] Chromosome.

[b] Peak genetic position with the greatest logarithm of odds (LOD).

[c] The 1.5-LOD confidence interval of QTL.

[d] Phenotypic variation explained (PVE) by the additive effects of the mapped QTL.

[e] Additive effect of the identified QTL: a positive value indicates that the Z58 allele increased trait expression, and a negative value indicates that the HD568 allele increased expression.

Additional Files

Additional file 1 Summary for phenotypic variation explained by each unconditional quantitative trail locus (QTL) at each stage.

Additional file 2 Summary for additive effect of each unconditional quantitative trail locus (QTL) at each stage.

Additional file 3 Summary of broad sense heritability for five traits at each stage.

Additional file 4 Summary of analysis of variance for five traits at each stage.

Figures

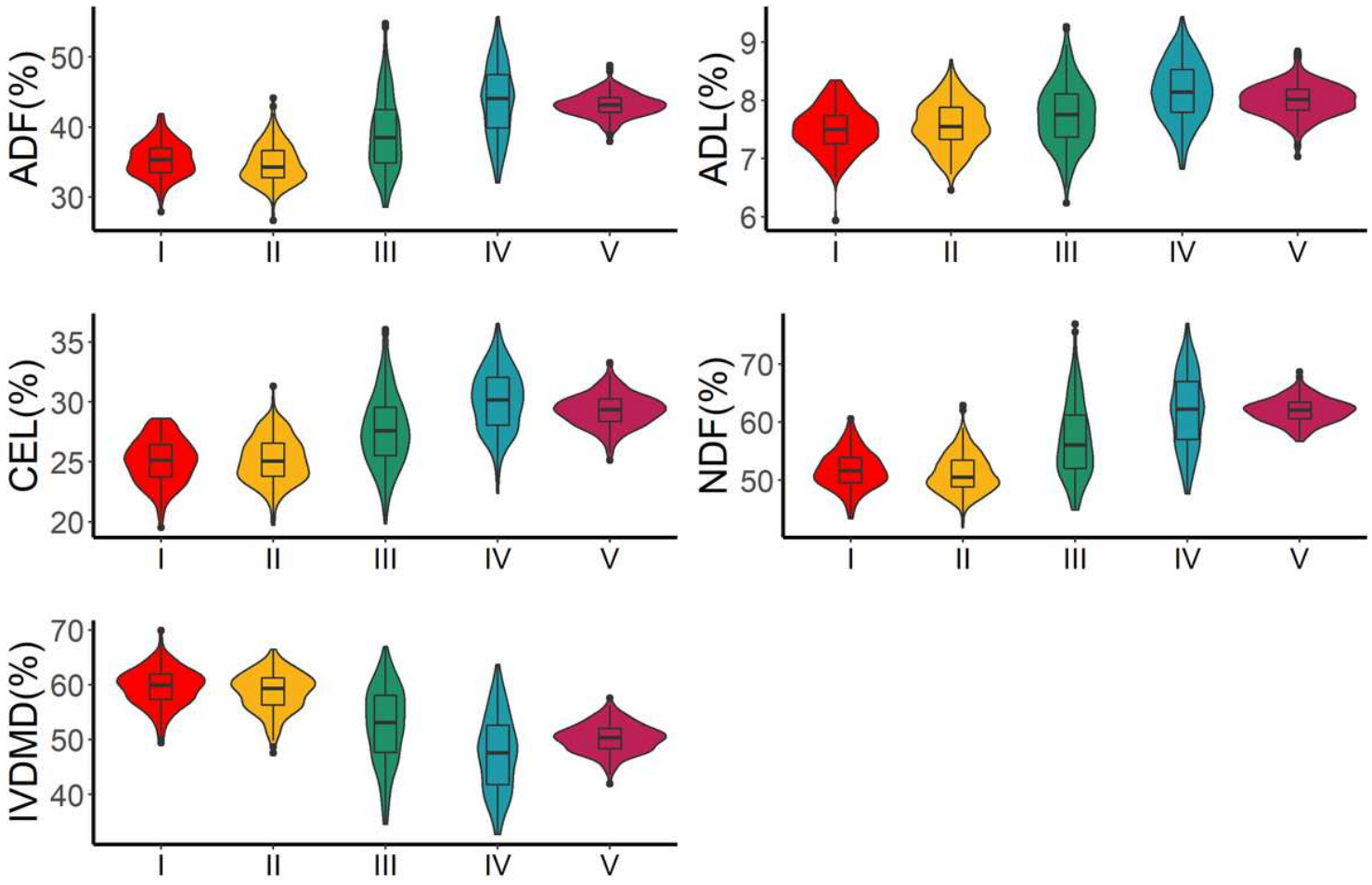

Figure 1

Changes in cell wall components and digestibility traits after silking in a recombinant inbred line (RIL) population. ADF, acid detergent fiber; ADL, acid detergent lignin; CEL, cellulose; NDF, neutral detergent fiber; IVDMD, in vitro dry matter digestibility. I–V represent 10–50 days after silking, respectively.

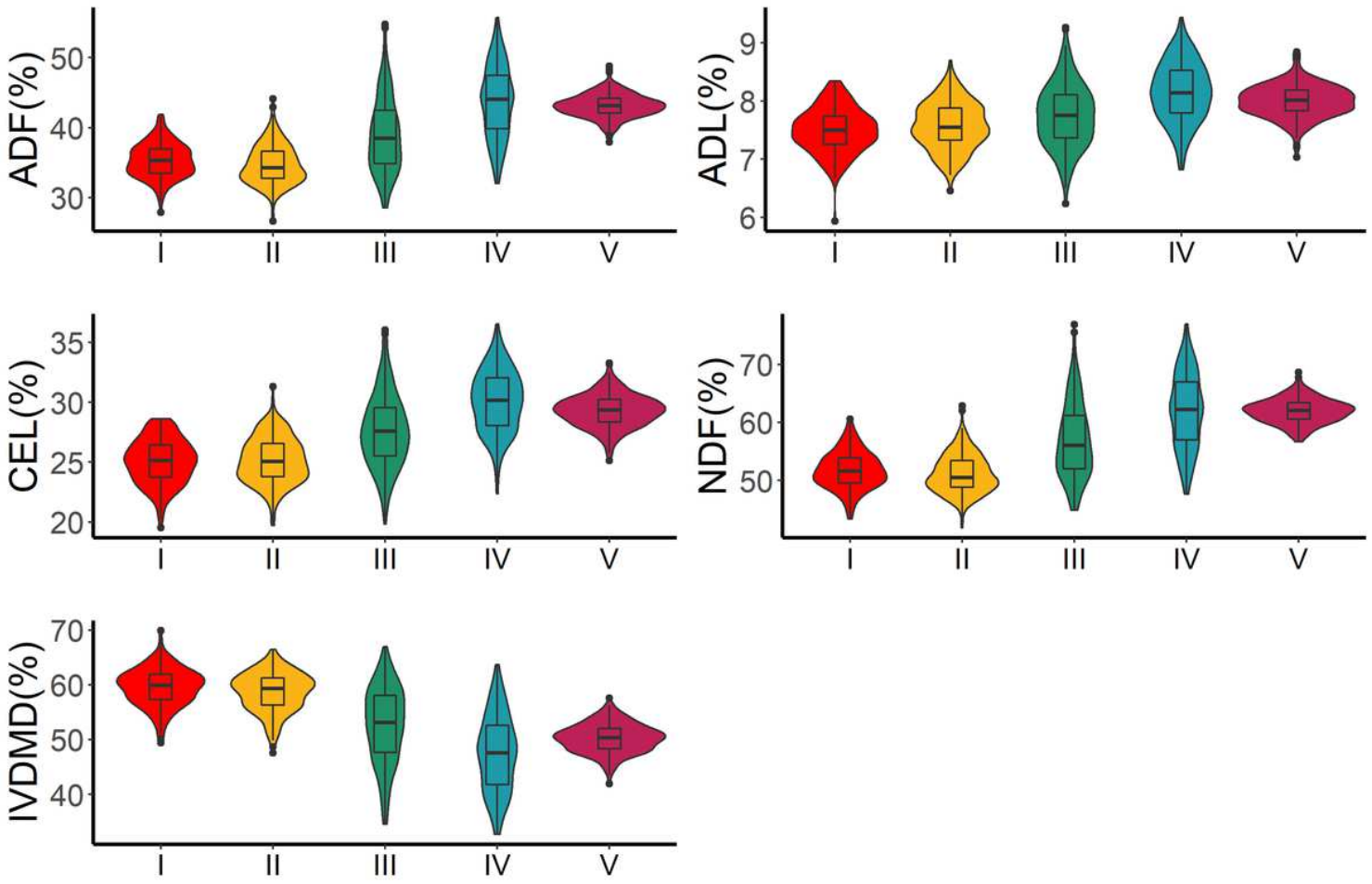

Figure 1

Changes in cell wall components and digestibility traits after silking in a recombinant inbred line (RIL) population. ADF, acid detergent fiber; ADL, acid detergent lignin; CEL, cellulose; NDF, neutral detergent fiber; IVDMD, in vitro dry matter digestibility. I–V represent 10–50 days after silking, respectively.

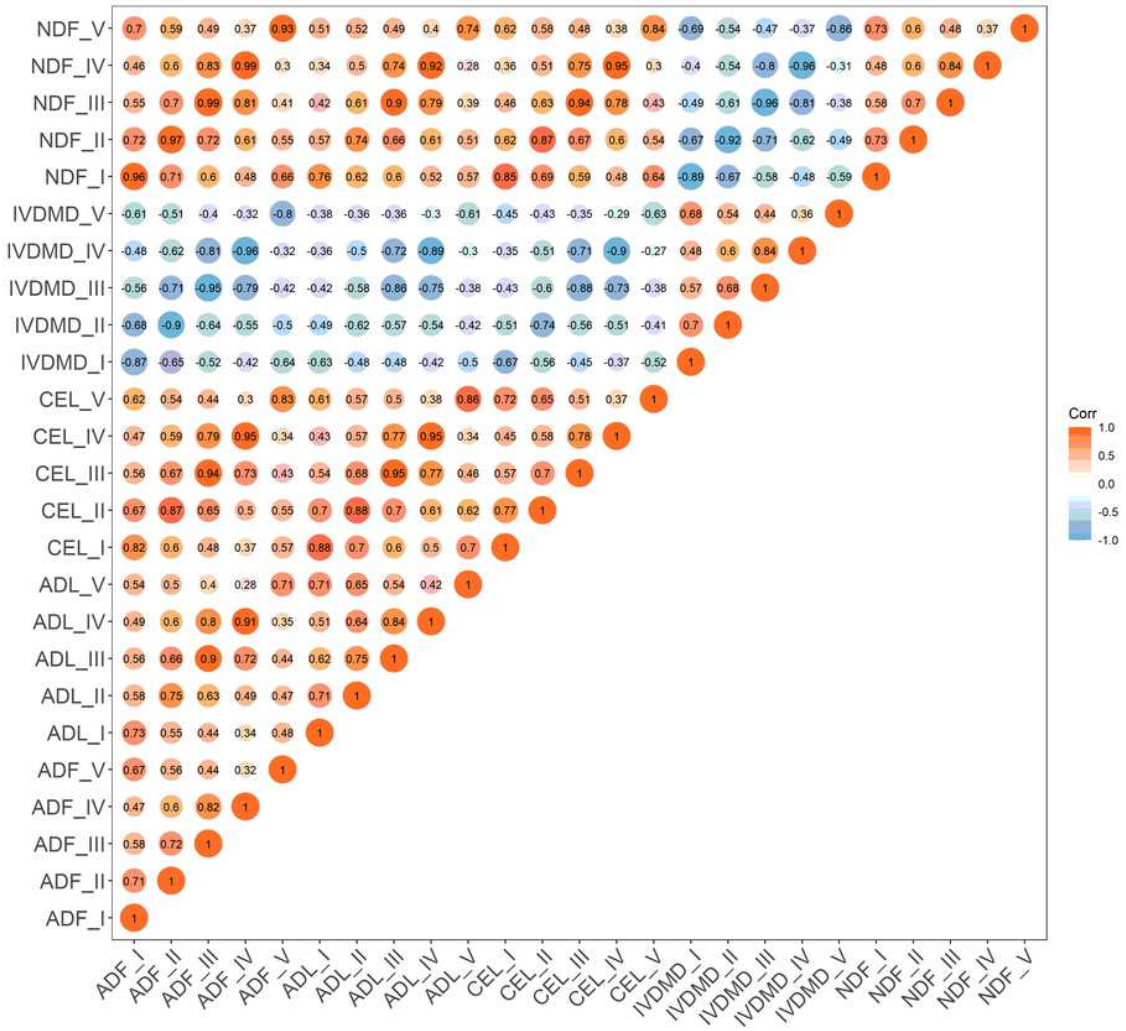

Figure 2

Correlation coefficients among acid detergent fiber (ADF), neutral detergent fiber (NDF), cellulose (CEL), acid detergent lignin (ADL), and in vitro dry matter digestibility (IVDMD) across five stages.

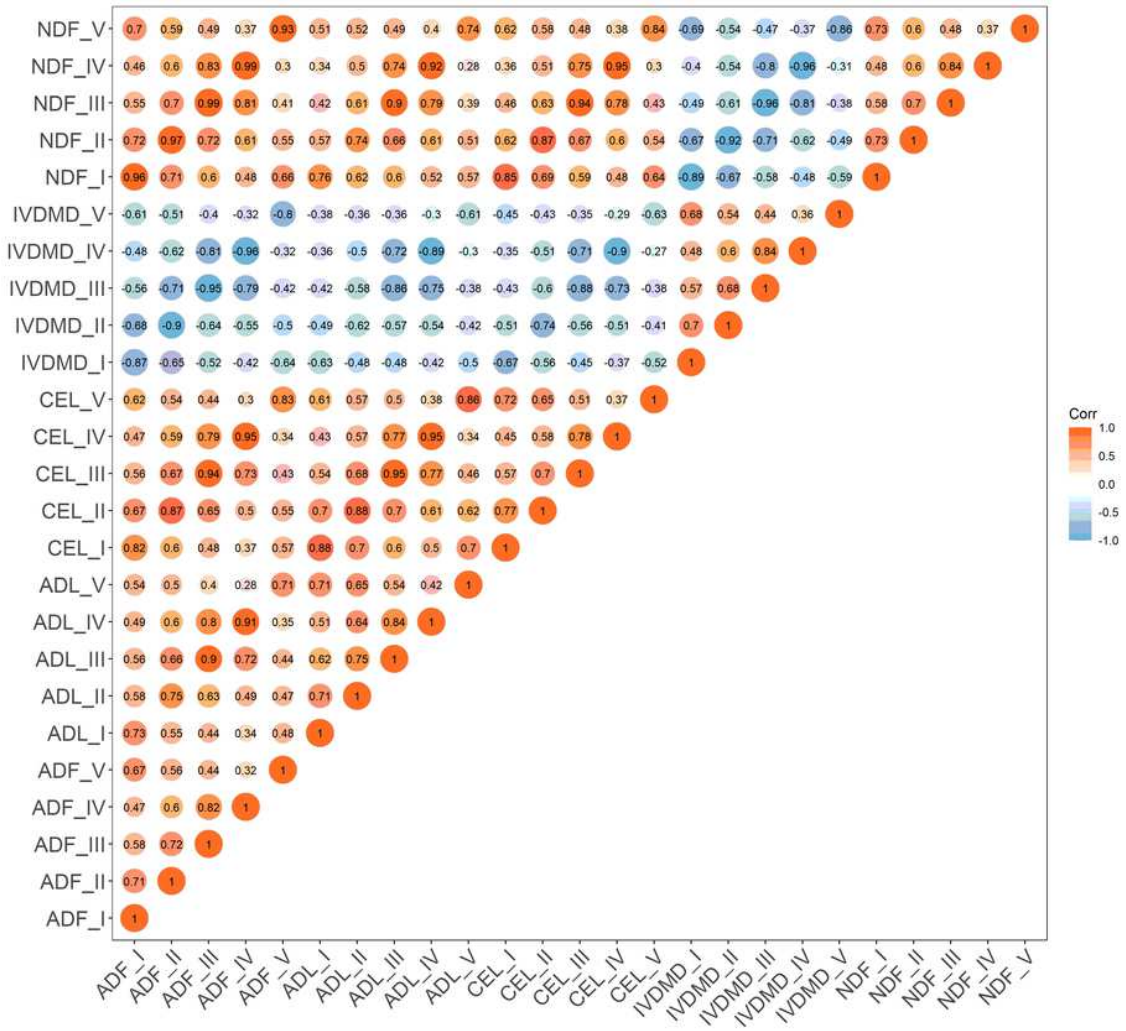

Figure 2

Correlation coefficients among acid detergent fiber (ADF), neutral detergent fiber (NDF), cellulose (CEL), acid detergent lignin (ADL), and in vitro dry matter digestibility (IVDMD) across five stages.

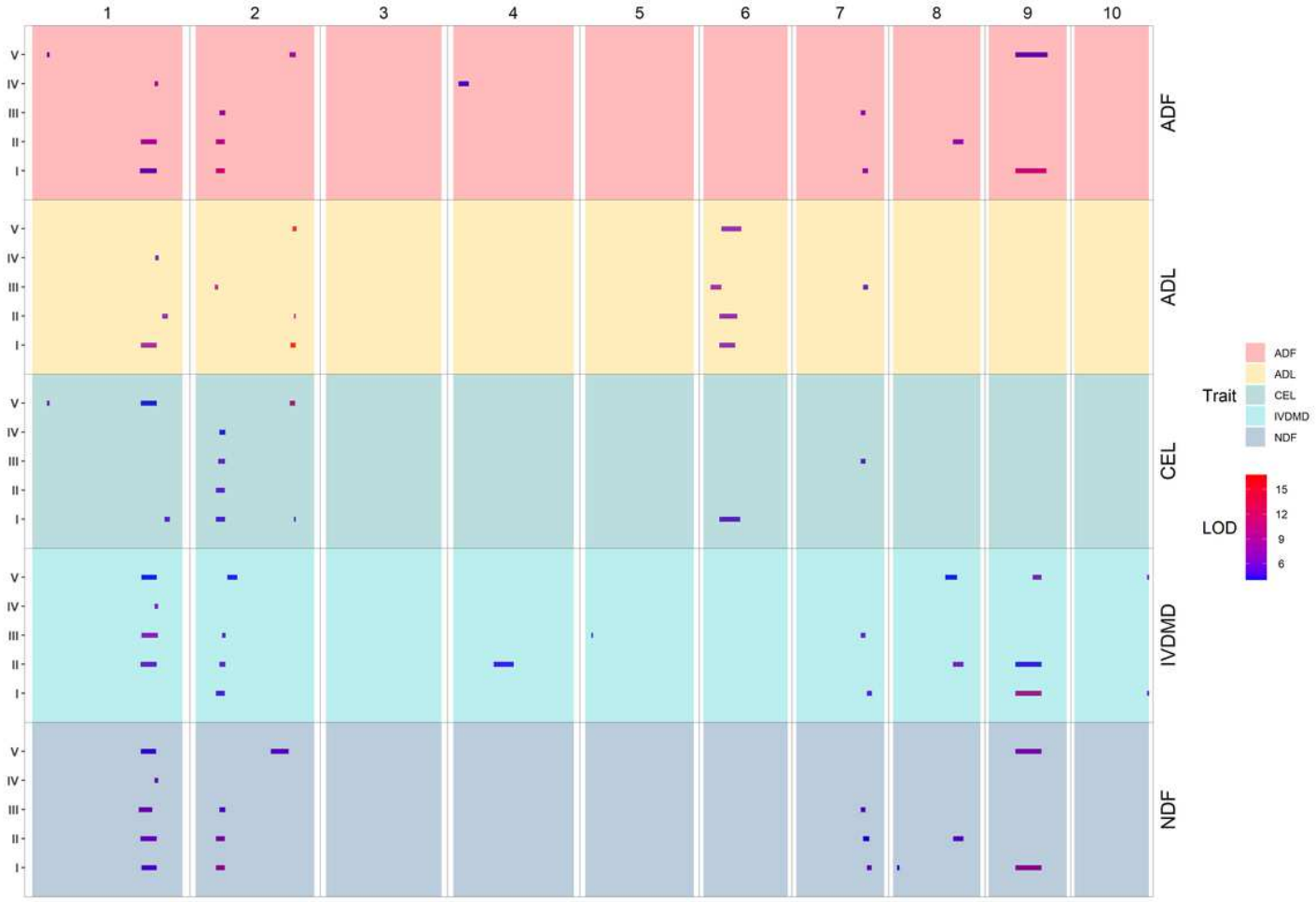

Figure 3

Chromosomal locations of quantitative trail loci (QTL) for cell wall components and digestibility traits in a maize recombinant inbred line (RIL) population.

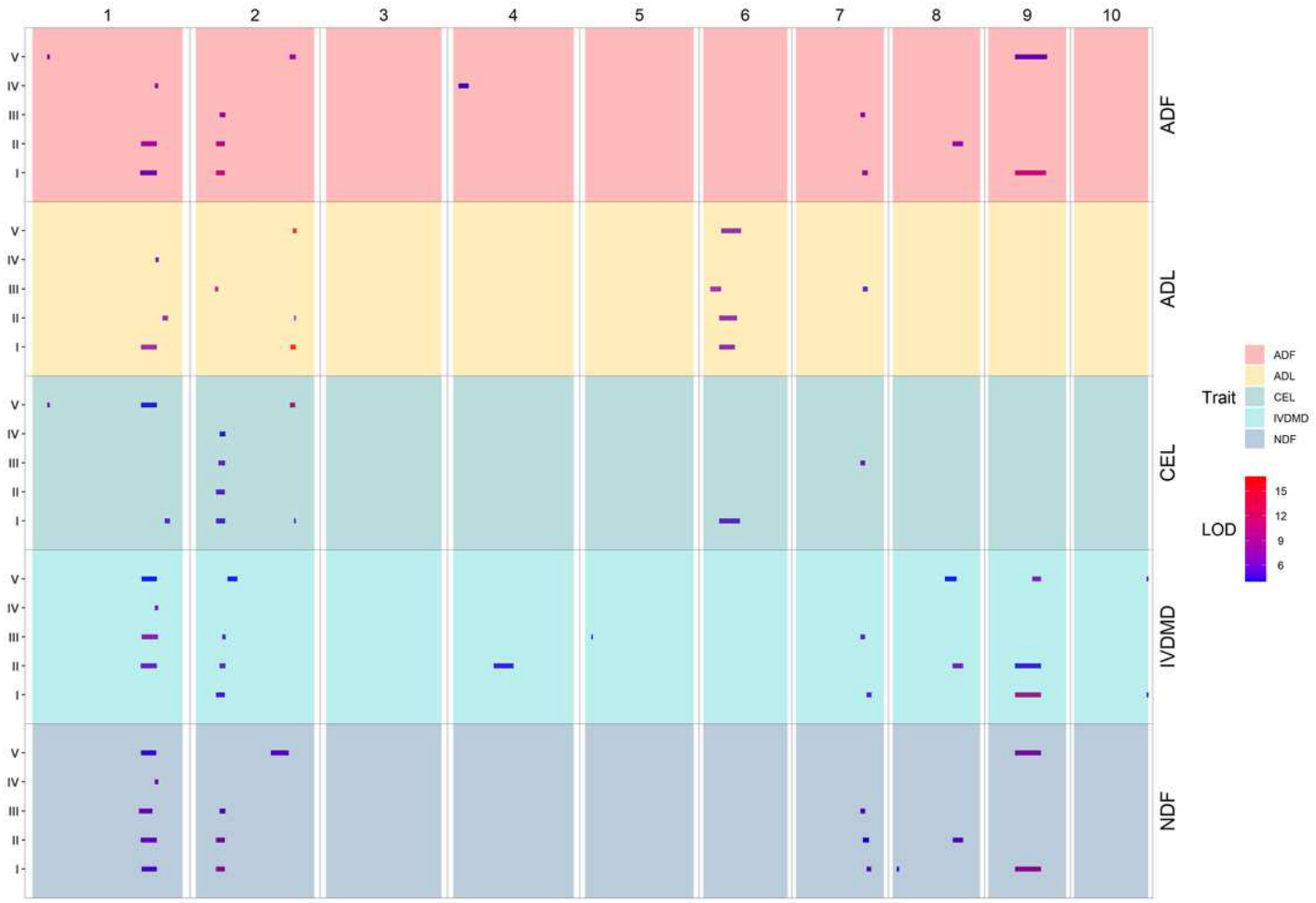

Figure 3

Chromosomal locations of quantitative trail loci (QTL) for cell wall components and digestibility traits in a maize recombinant inbred line (RIL) population.

Supplementary Files

This is a list of supplementary files associated with this preprint. Click to download.

- Additionalfile1.tif
- Additionalfile2.tif
- Additionalfile3.xlsx
- Additionalfile4.xlsx